

---

---

# Brown Adipose Tissue: A Protective Mechanism Against “Preprediabetes”?

John P. Crandall, Tyler J. Fraum, and Richard L. Wahl

*Mallinckrodt Institute of Radiology, Washington University School of Medicine, St. Louis, Missouri*

---

See an invited perspective on this article on page 1431.

---

Brown adipose tissue (BAT) is present in a significant number of adult humans and has been postulated to exert beneficial metabolic effects. Lean, nondiabetic patients undergoing clinical PET/CT imaging are more likely to exhibit incidental BAT activation. The aim of this study was to assess metabolic changes associated with the cold activation of BAT and to compare baseline blood metabolites in participants with varying amounts of active BAT. **Methods:** Serum blood samples were collected from healthy adult volunteers (body mass index, 18.0–25.0, and age  $\leq$  35 y) before and after 2 h of exposure to cold.  $^{18}\text{F}$ -FDG PET/CT imaging was performed immediately after cold exposure. Activated BAT was segmented, and fasting glucose, insulin, lipid, and other blood metabolite levels were correlated with volume and intensity of active BAT. Using a median cutoff, subjects were classified as high-BAT (BAT<sub>high</sub>) or low-BAT (BAT<sub>low</sub>). **Results:** A higher volume of activated BAT was associated with significantly higher precooling glucose and insulin levels ( $P < 0.001$  for each). Precooling thyroid-stimulating hormone and triglyceride levels were significantly higher in the BAT<sub>high</sub> than the BAT<sub>low</sub> group ( $P = 0.002$  and  $P < 0.001$ , respectively). Triglyceride levels tended to increase over the cooling period in both BAT groups but increased significantly more in the BAT<sub>high</sub> group ( $15.7 \pm 13.2$  mg/dL;  $P < 0.001$ ) than in the BAT<sub>low</sub> group ( $4.5 \pm 12.2$  mg/dL;  $P = 0.061$ ). **Conclusion:** These findings may indicate that BAT is recruited to counteract incipient “preprediabetic” states, potentially serving as a first-line protective mechanism against very early metabolic or hormonal variations.

**Key Words:** endocrine; molecular imaging; PET/CT; brown fat; FDG; metabolism

J Nucl Med 2022; 63:1433–1440

DOI: 10.2967/jnumed.121.263357

---

**B**rown adipose tissue (BAT) uses a variety of metabolic substrates to produce heat in mammals and so constitutes a potential target for the treatment of obesity and other metabolic disorders (1). White adipose tissue (WAT) stores energy as triacylglycerols, which can be released as nonesterified fatty acids (NEFAs) for energy consumption by metabolically active organs. BAT uses fatty acids released from intracellular triglyceride stores for  $\beta$ -oxidation to generate heat by a process known as adaptive thermogenesis (2).

The presence of BAT in adult humans was initially recognized mainly on  $^{18}\text{F}$ -FDG PET/CT examinations performed for oncologic indications (3,4).  $^{18}\text{F}$ -FDG PET has since become the most commonly used technique for the in vivo detection of cold-activated BAT in humans (5,6). Studies using PET with  $^{18}\text{F}$ -FDG or fatty-acid tracers have demonstrated that BAT consumes glucose and fatty acids (7–9).

Two primary pathways are known to regulate BAT glucose metabolism: adrenergic and insulin signaling (1). On sympathetic nervous system activation, norepinephrine is released, which binds to adrenergic receptors ( $\beta_1$ -,  $\beta_2$ -, and  $\beta_3$ -adrenoceptors) expressed on BAT cell surfaces, causing an increase in cytosolic cyclic adenosine monophosphate levels (10). The result is an increase in glucose transporter 1 transcription and, via activation of the mammalian target of rapamycin complex 2, the translocation of this newly synthesized glucose transporter 1 to the cell membrane (11). Alternatively, insulin binds to BAT insulin receptors, and phosphoinositide 3-kinases phosphorylate protein kinase B, inducing the translocation of glucose transporter 4 to the cell membrane. Glucose, having been taken up by BAT cells using either pathway, is used for glycolysis, maintaining fatty acid oxidation, or activation of uncoupling protein 1 via de novo lipogenesis and fatty-acid synthesis (2).

The regulation of glucose by activated BAT may have important therapeutic implications, as exposure to cold has been shown to reverse glucose intolerance and insulin resistance in animal models (12–14). Cold acclimation may also result in increased fractional uptake in BAT (15). Observational human studies have indicated that the presence of active BAT is associated with lower glucose levels and a decreased risk of diabetes (16–18). However, the role of BAT in whole-body glucose consumption remains unclear since several prospective studies have indicated a minimal contribution by BAT to systemic glucose utilization (8,19). Still, others have shown a protective effect of BAT against diabetes (20).

Current evidence indicates that lipid metabolism in humans is modulated, at least to some degree, by BAT. BAT activation has been correlated with cold-induced increases in WAT lipolysis and NEFA oxidation, indicating that NEFAs are mobilized from WAT to fuel activated BAT. It has been hypothesized that increased BAT activity or volume increases uptake of NEFAs in BAT, improving overall lipid metabolism (12,21). A recent retrospective study found that nonstimulated BAT was associated with lower concentrations of circulating triglycerides (22). Rodent studies have demonstrated the clearance of triglyceride-rich lipoproteins and cholesterol from circulation by BAT (12,23) and have even seemed to demonstrate that active BAT modulates fuel selection in non-BAT organs (24). Even during fasting and postprandial conditions, BAT has been shown to take up significant amounts of circulating free fatty acids in mice (25). However, the practical implications of active BAT on lipid metabolism in humans remain unclear (26,27).

---

Received Dec. 4, 2021; revision accepted Mar. 21, 2022.

For correspondence or reprints, contact Richard L. Wahl (rwahl@wustl.edu).

Published online Apr. 7, 2022.

COPYRIGHT © 2022 by the Society of Nuclear Medicine and Molecular Imaging.

The primary aim of this study was to assess whether there are differences in baseline glucose, insulin, lipid, and other metabolite levels between subjects with varying amounts of cold-activated BAT. A secondary aim was to evaluate changes in these blood markers between precooling and postcooling serum blood samples. An additional aim was to assess how different lifestyle parameters are associated with BAT volume. These data were collected as part of a prospective study assessing the repeatability of BAT activity levels on  $^{18}\text{F}$ -FDG PET/CT (28).

## MATERIALS AND METHODS

This prospective study was approved by the Washington University Institutional Review Board. All subjects provided written informed consent before participation. Between March 2016 and January 2020, 34 healthy volunteers were enrolled and underwent  $^{18}\text{F}$ -FDG PET/CT imaging after a cooling procedure intended to activate BAT (subject characteristics provided in Table 1). The median  $^{18}\text{F}$ -FDG uptake time was 61.0 min, with a range of 59.0–76.6 min. Median blood glucose, measured immediately before  $^{18}\text{F}$ -FDG administration, was 78 mg/dL, and the range was 58–103 mg/dL. Since younger age and lower body mass index have been shown to correlate with higher amounts of metabolically active BAT (7,29,30), healthy adult volunteers aged 18–35 with a body mass index between 18 and 25 were eligible for this study. Furthermore, as drugs targeting the sympathetic nervous system (e.g., nicotine,  $\beta$ -blockers, and amphetamines) can interfere with BAT activation (31), individuals with a history of consuming these agents were excluded. A complete list of inclusion and exclusion criteria can be found in Supplemental Table 1 (supplemental materials are available at <http://jnm.snmjournals.org>). Subjects were recruited using flyers posted at various locations on the Washington University in St. Louis medical campus.

### Subject Preparation

A schematic representation of the imaging visit is shown in Figure 1. All subjects were instructed to fast for at least 6 h before imaging and to avoid high-carbohydrate and high-fat foods. Subjects were also asked to

avoid cold exposure and to refrain from exercise during the 24 h before the imaging sessions. To prevent premature BAT activation, subjects were kept warm for 60 min, using warmed blankets, before the start of the cold-exposure procedure. During this period, the precooling blood sample was drawn for metabolite analysis. After the preparatory phase, participants were outfitted in a cooling suit (CureWrap; MRTE Advanced Technologies) that circulates chilled water at a set temperature.

### Lifestyle Interview

During the preparatory phase, subjects were asked a series of questions to assess the impact of lifestyle on BAT activity. Volunteers were asked to describe any specific diet they followed within the year before the study, to report any dietary supplements they consume regularly, and to estimate their weekly caffeine and alcohol intake. Subjects were asked to describe their normal exercise habits, if any, during the previous year. Exercise descriptions were recorded and coded as mostly aerobic, mostly anaerobic, or combination aerobic/anaerobic.

### Cooling Protocol

An individualized cooling protocol was used with a goal of cooling the subject to just above the shivering point (5). Initially, the water temperature of the cooling suit was set at 10°C for all subjects. Subjects were monitored for shivering, both visibly and via electromyogram (electrodes placed over the vastus lateralis, pectoralis major, and latissimus dorsi muscles). If shivering was observed or reported, the water temperature was increased at 0.5°C increments every 60 s until shivering stopped. Oral temperature and blood pressure were measured every 5 min during the cooling procedure. A 185-MBq dose of  $^{18}\text{F}$ -FDG was administered intravenously after 60 min of cooling. Cooling continued during the 60-min  $^{18}\text{F}$ -FDG uptake phase. Immediately before  $^{18}\text{F}$ -FDG PET/CT imaging, subjects were removed from the cooling suit.

### Imaging Protocol

Imaging and reconstruction parameters are detailed in Supplemental Table 2. All subjects were imaged on a Biograph 40 PET/CT TruePoint/TrueView scanner (Siemens AG). In humans, most active BAT depots are located in the supraclavicular and paravertebral regions, with additional foci commonly seen in the axillary, intercostal, mediastinal, and perirenal areas. Therefore, PET imaging (three 8-min list-mode acquisitions) was performed from the skull base to the umbilicus. A low-dose CT scan (using CARE Dose [Siemens] tube current modulation) was obtained immediately before the PET scan. The imaging protocol followed the standards set forth by the Uniform Protocols for Imaging in Clinical Trials for  $^{18}\text{F}$ -FDG PET/CT and the Radiologic Society of North America–Quantitative Imaging Biomarker Alliance’s profile for quantitative  $^{18}\text{F}$ -FDG PET/CT (32,33).

### Image Analysis

Images were analyzed using MIM, version 6.9.3 (MIM Software). Activated BAT was segmented (Fig. 2) and quantified according to the recommendations of version 1.0 of the Brown Adipose Reporting Criteria in Imaging Studies (5). Areas known to contain BAT were qualitatively assessed, and likely BAT depots were identified. Volumes of interest were drawn on coronal  $^{18}\text{F}$ -FDG PET/CT images slice-by-slice, taking care not to include any adjacent normal  $^{18}\text{F}$ -FDG-avid tissues. Thresholds were then applied to this manual volume of interest to first remove voxels with lean body mass-adjusted SUVs (SULs) below 1.2 and then to remove voxels with Hounsfield units outside the  $-190$  to  $-10$  range. Thus, the final activated BAT volumes consisted of voxels with SULs above normal background levels and within the fat density range.

The total activated BAT metabolic volume (BMV) was the sum of all segmented BAT volumes. For participants included in the test-retest study, BMV and the maximum SUL (SUL<sub>max</sub>) for each imaging session were analyzed separately. The SUL<sub>max</sub> was defined as the

**TABLE 1**  
Subject Characteristics

Characteristic	Total	BAT <sub>high</sub>	BAT <sub>low</sub>
<b>Sex</b>			
Male	7	4	3
Female	34	17	17
Age (y)	23.8 ± 3.5	23.2 ± 2.7	24.7 ± 4.3
Height (m)	1.66 ± 0.09	1.67 ± 0.09	1.65 ± 0.09
Weight (kg)	62.3 ± 8.8	64.6 ± 9.1	59.6 ± 7.9
Body mass index (kg/m <sup>2</sup> )	22.3 ± 1.8	23.0 ± 1.7	21.6 ± 1.5
<b>Race</b>			
White	20	12	8
Black	2	0	2
Asian	12	5	7
<b>Ethnicity</b>			
Hispanic		1	1
Non-Hispanic	32	16	16

Qualitative data are number; continuous data are mean ± SD

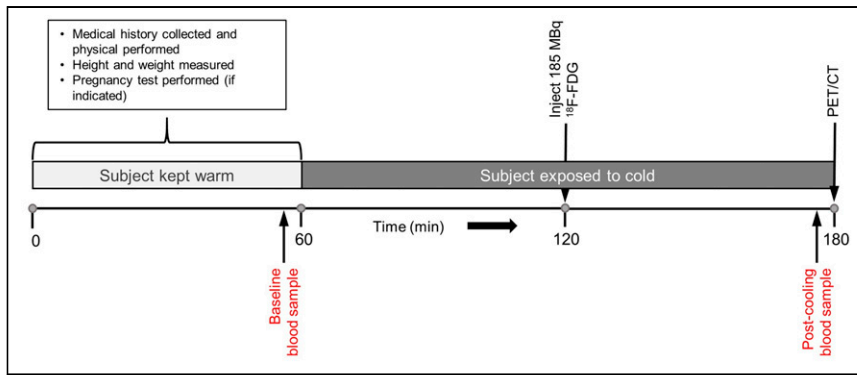


**FIGURE 1.** BAT activation and imaging process. After 1-h warming period, volunteers were exposed to cold for ~2 h to activate BAT. After first hour of cooling, 185 MBq of  $^{18}\text{F}$ -FDG were administered intravenously. Cooling continued for a second hour, and PET/CT imaging was performed immediately afterward.

single voxel within all the segmented BAT depots with the greatest  $^{18}\text{F}$ -FDG uptake. The version of MIM used for our analyses uses the James equation for lean body mass computation (34). For subjects without visually detectable BAT, the  $\text{SUL}_{\text{max}}$  was instead based on the background activity of the fat in the right supraclavicular fossa, using a spheric region of interest (3.0-cm radius). This region was chosen because the supraclavicular fossa most commonly contains the BAT depot with the most  $^{18}\text{F}$ -FDG uptake.

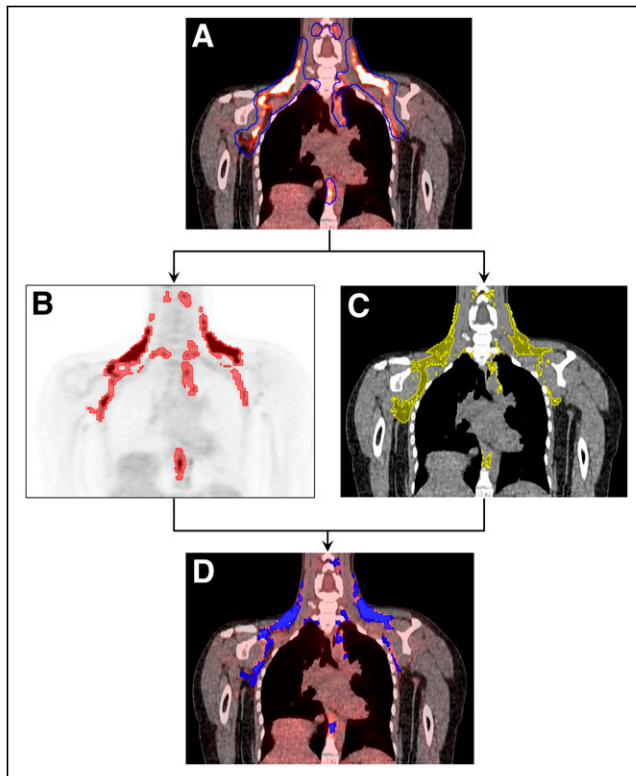


**FIGURE 2.** BAT segmentation was performed per Brown Adipose Reporting Criteria in Imaging Studies, version 1.0, guidelines. (A) Areas known to contain BAT depots were manually delineated. (B and C) On PET images, voxels with  $\text{SUL}_{\text{max}}$  less than 1.2 were removed (B) and on CT images, voxels with Hounsfield units outside range of  $-190$  to  $-10$  were removed (C). (D) Boolean intersection of PET and CT images was used to obtain final volumes of interest.

## Biologic Assays

Methods used for blood sample analyses are provided in Supplemental Table 3. All tests were performed using either Cobas 6000 or Cobas 8000 (Roche Diagnostics). Blood samples were analyzed in the Barnes Jewish Clinical Chemistry Laboratory, which holds College of American Pathologists and Clinical Laboratory Improvement Amendments certifications. Lipid data were available for all subjects, whereas insulin, glucose, and other metabolite data were available for only a subset of participants.

## Statistics

Numeric results are reported as mean and SD or as median and interquartile range. Subject characteristics were summarized descriptively via means, medians, SD, and ranges.

A subset of participants was included in a test-retest repeatability study ( $n = 29$ ) and underwent the cooling and imaging protocol twice on separate days. Blood samples collected during these visits were pooled with the remaining data and considered independent samples. Baseline and postcooling metabolite measurements were compared using paired  $t$  tests. Serum metabolite differences between high-BAT ( $\text{BAT}_{\text{high}}$ ) and low-BAT ( $\text{BAT}_{\text{low}}$ ) groups were assessed using unpaired  $t$  tests or Mann-Whitney  $U$  tests, depending on group normality. Group normality was assessed using D'Agostino-Pearson tests. The Fisher exact test was used to assess differences in demographics and lifestyle assessments between subjects without versus with detectable BAT. Data were analyzed using R, version 4.0.3 (<http://cran.r-project.org/>), and Excel, version 2016 (Microsoft Corp.). A  $P$  value of less than 0.05 was considered significant, unless otherwise indicated. A Bonferroni adjustment for multiple comparisons was applied when necessary to control for type I errors.

## RESULTS

### Subject Characteristics

During cold exposure, oral temperatures varied by a mean of  $\pm 0.4^\circ\text{C}$ . Systolic pressure increased during cooling by a minimum of 8 mm Hg and a maximum of 42 mm Hg. Diastolic pressure increased during cooling by a minimum of 11 mm Hg and a maximum of 39 mm Hg. Heart rate increased by 11–30 beats per minute throughout cooling.

Activated BAT was detected in 28 of 34 (82.4%) subjects. Using a median volume cutoff, PET/CT studies showing an activated BMV greater than or less than  $120\text{ cm}^3$  were classified as  $\text{BAT}_{\text{high}}$  or  $\text{BAT}_{\text{low}}$ , respectively. The mean BMV of the  $\text{BAT}_{\text{low}}$  group ( $n = 17$ ) was  $36.9 \pm 29.1\text{ cm}^3$ , and the mean BMV of the  $\text{BAT}_{\text{high}}$  group ( $n = 17$ ) was  $224.3 \pm 78.4\text{ cm}^3$ . There were no substantial differences in age, height, or weight between groups. A significant difference in body mass index was found, with  $\text{BAT}_{\text{high}}$  subjects having a higher body mass index than  $\text{BAT}_{\text{low}}$  subjects ( $P = 0.026$ ).

### Insulin and Glucose

Mean baseline insulin and glucose levels were significantly lower in the  $\text{BAT}_{\text{low}}$  than the  $\text{BAT}_{\text{high}}$  group (Table 2). Between baseline and postcooling samples, mean insulin levels increased by  $1.6 \pm 1.2\text{ }\mu\text{IU/mL}$  in the  $\text{BAT}_{\text{low}}$  group and decreased by  $2.7 \pm 1.4\text{ }\mu\text{IU/mL}$  in the  $\text{BAT}_{\text{high}}$  group. Baseline glucose and insulin showed significant positive correlations with both BMV and  $\text{SUL}_{\text{max}}$  (Figs. 3 and 4). The change in glucose and insulin levels from baseline to postcooling samples showed significant negative correlations with both

**TABLE 2**  
Glucose and Insulin *t* Test and Regression Analysis Results

Metabolite	Time point	$\mu$ (BAT <sub>low</sub> )	$\sigma$	$\mu$ (BAT <sub>high</sub> )	$\sigma$	<i>r</i> (BMV)	<i>r</i> (SUL <sub>max</sub> )	<i>P</i>
Insulin ( $\mu$ IU/mL)	Baseline	3.3	0.8	8.7	3.0	0.90	0.74	<0.001
	Postcooling	4.9	1.9	6.1	2.6	0.71	0.43	0.327
	Change	1.6	1.2	-2.7	1.4	-0.79	-0.64	<0.001
Glucose (mg/dL)	Baseline	70.8	10.2	88.3	11.4	0.59	0.54	<0.001
	Postcooling	84.3	12.3	85.2	7.3	0.12	0.06	0.815
	Change	3.0	5.6	-3.1	5.5	-0.58	-0.54	0.013

*P* values were generated using unpaired *t* tests comparing BAT<sub>high</sub> and BAT<sub>low</sub> groups. Using Bonferroni adjustment, *P* < 0.025 was considered significant.

BMV and SUL<sub>max</sub>. Baseline insulin and glucose also significantly correlated with one another (*r* = 0.67; *P* < 0.001), as were the changes in insulin and glucose (*r* = 0.51; *P* = 0.019).

### Lipids

Groupwise serum lipid results are shown in Table 3. Baseline total cholesterol, triglycerides, and high-density lipoprotein were significantly higher (*P* = 0.002, *P* < 0.001, and *P* = 0.004, respectively) in BAT<sub>low</sub> versus BAT<sub>high</sub> subjects. The BAT<sub>low</sub> group also showed higher baseline low-density lipoprotein and non-high-density lipoprotein levels than the BAT<sub>high</sub> group, though not statistically different. Between baseline and postcooling blood samples, serum total cholesterol, high-density lipoprotein, non-high-density lipoprotein, and low-density lipoprotein increased significantly for both groups (all *P* values below 0.01). Serum triglycerides increased significantly between baseline and postcooling samples for BAT<sub>high</sub>

subjects ( $15.7 \pm 13.2$  mg/dL; *P* < 0.001) but did not increase significantly in the BAT<sub>low</sub> group ( $4.5 \pm 12.2$  mg/dL; *P* = 0.061).

Baseline triglycerides, cholesterol, and high-density lipoprotein also significantly correlated with BMV and SUL<sub>max</sub> (Supplemental Figs. 1 and 2). The change in triglycerides from baseline to postcooling samples also significantly correlated with BMV and SUL<sub>max</sub>.

### Other Metabolites

Several additional metabolites showed groupwise differences and varied significantly between baseline and postcooling blood samples (Table 4). Mean baseline thyroid-stimulating hormone (TSH) was significantly lower in the BAT<sub>low</sub> than the BAT<sub>high</sub> group (*P* = 0.002). Mean baseline sodium, anion gap, urea nitrogen, albumin, and alkaline phosphatase were significantly higher in the BAT<sub>low</sub> than the BAT<sub>high</sub> group.

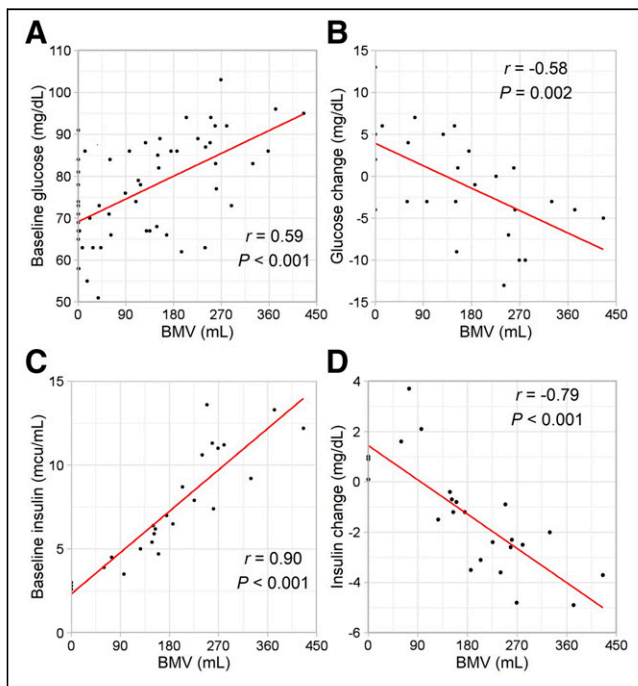


**FIGURE 3.** Regression analysis shows correlation between BMV and baseline serum glucose (A), change in glucose from baseline to postcooling (B), baseline serum insulin (C), and change in insulin (D). Baseline values were subtracted from postcooling values.

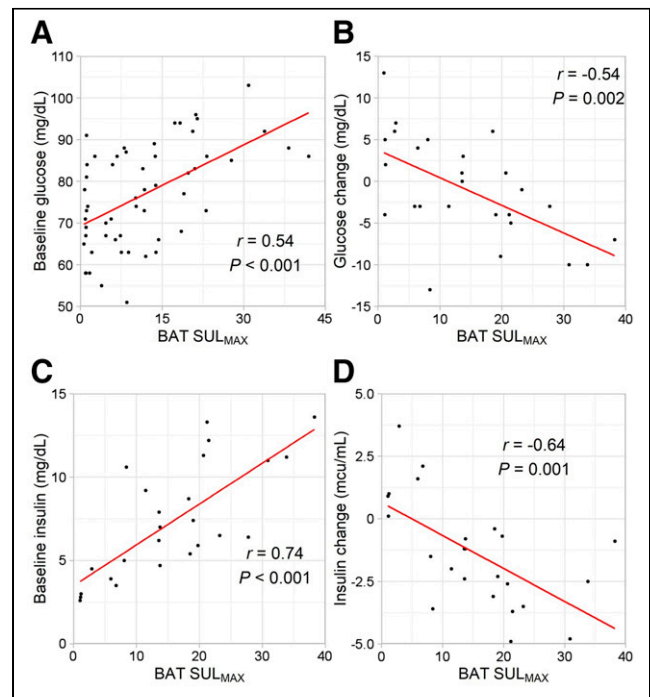


**FIGURE 4.** Regression analysis shows correlation between BAT SUL<sub>max</sub> and baseline serum glucose (A), change in glucose from baseline to postcooling (B), baseline serum insulin (C), and change in insulin (D). Baseline values were subtracted from postcooling values.

**TABLE 3**  
Serum Lipid *t* Test and Regression Analysis Results

Lipid	Time point	BAT <sub>low</sub>		BAT <sub>high</sub>		<i>r</i>		<i>P</i>
		$\mu$	$\sigma$	$\mu$	$\sigma$	BMV	SUL <sub>max</sub>	
Cholesterol (mg/dL)	Baseline	164.0	34.0	141.9	19.8	-0.43	-0.42	0.002
	Postcooling	174.0	32.4	156.0	21.2	-0.34	-0.34	0.010
	Change	9.0	11.0	14.9	7.9	0.33	0.26	0.023
Triglycerides (mg/dL)	Baseline	63.6	24.1	89.6	26.7	0.56	0.45	<0.001
	Postcooling	66.5	24.5	105.7	31.2	0.60	0.48	<0.001
	Change	4.5	12.2	15.7	13.2	0.45	0.34	<0.001
High-density lipoprotein (mg/dL)	Baseline	66.5	14.4	56.0	16.4	-0.41	-0.35	0.004
	Postcooling	70.6	13.6	62.4	20.9	-0.28	-0.22	0.181
	Change	3.4	4.9	6.4	12.0	0.21	0.23	0.231
Low-density lipoprotein (mg/dL)	Baseline	83.7	28.9	73.8	21.3	-0.16	-0.23	0.058
	Postcooling	86.4	26.8	80.7	22.3	-0.11	-0.15	0.173
	Change	-0.9	29.2	7.5	9.1	0.15	0.16	0.153
Non-high-density lipoprotein (mg/dL)	Baseline	97.2	29.5	89.2	19.5	-0.14	-0.19	0.093
	Postcooling	103.6	29.8	97.8	20.3	-0.13	-0.17	0.182
	Change	6.1	7.7	9.2	8.3	0.02	0.06	0.185

*P* values were generated using unpaired *t* tests comparing BAT<sub>high</sub> and BAT<sub>low</sub> groups. Using Bonferroni adjustment, *P* < 0.010 was considered significant.

### Lifestyle

Participants reported engaging in either no strict dietary regimen or adhering to a vegetarian, vegan, gluten-free, low-carbohydrate, or pescatarian diet. BAT<sub>low</sub> subjects were significantly more likely to report observing a controlled diet than BAT<sub>high</sub> subjects (*P* = 0.007). Only 1 of 17 BAT<sub>high</sub> participants reported following a specific diet (pescatarian), whereas 8 of 17 BAT<sub>low</sub> subjects reported adhering to a strict diet. The use of dietary supplements also varied between groups, with BAT<sub>high</sub> subjects reporting either no use of dietary supplements or use of protein, melatonin, biotin, omega-6 fatty acids, or magnesium (8/17 subjects), whereas BAT<sub>low</sub> subjects reported either no diet supplementation or using only a daily multivitamin (7/17 subjects). There were no significant differences between groups with respect to self-reported weekly intake of caffeine or alcohol.

Exercise habits also differed between groups. Those who reported not regularly exercising were significantly more likely to have higher BAT volumes (7/17 BAT<sub>high</sub> vs. 0/16 BAT<sub>low</sub>; *P* = 0.018). Among those who exercised regularly, the self-reported mean number of hours spent exercising per week was 3.4 in the BAT<sub>low</sub> group and 1.9 in the BAT<sub>high</sub> group (*P* = 0.011). Within the BAT<sub>low</sub> group, 1 participant reported engaging in mostly anaerobic exercise, 10 in mostly aerobic exercise, and 6 in exercise that incorporated aerobic and anaerobic elements. Three BAT<sub>high</sub> subjects reported engaging in mostly anaerobic exercise, 2 in mostly aerobic exercise, and 5 in exercise that was both aerobic and anaerobic.

### DISCUSSION

BAT has emerged as a potential therapeutic target for obesity and related metabolic diseases. Using a previously described method, BAT was activated in this study using cold exposure and then imaged using <sup>18</sup>F-FDG PET/CT. Higher baseline insulin and glucose levels correlated with higher BMV (Supplemental Fig. 3).

Greater declines in insulin and glucose levels after BAT activation also correlated with higher BMV.

### Glucose and Insulin Activity

Activated BAT has been shown to act as a glucose sink in both warm and cold conditions (35,36), which is consistent with the significant positive correlation seen here between BMV and decreases in glucose and insulin levels during cooling. BAT thermogenesis likely resulted in significant uptake of glucose in BAT, especially in subjects with higher amounts of BAT, consistent with previous studies. However, our results are inconsistent with studies showing increased BAT uptake of glucose during warm conditions, as baseline glucose and insulin both positively correlated with BMV in our subjects. Retrospective analyses have generally concluded that patients with active BAT are more likely to have lower fasting glucose levels and less likely to be diabetic (7,16,17,37,38). Though, as these observational studies consisted mostly of patients undergoing clinical <sup>18</sup>F-FDG PET/CT, the populations evaluated were mostly much older than the volunteers enrolled in the current study.

### Lipid Metabolism

The role of BAT in systemic lipid metabolism is supported by previous studies showing that the amount of detectable BAT correlates with cold-induced increases in WAT lipolysis and NEFA oxidation, suggesting that BAT activation plays a role in mobilization of NEFAs from WAT and their oxidative disposal in BAT (19,21). Din et al. found that in BAT regions, subjects with higher volumes of activated BAT took up more NEFAs from circulation than subjects with lower volumes of BAT (39). It has also been shown that administration of nicotinic acid, an inhibitor of triglyceride lipolysis, suppresses the cold-induced BAT metabolic rate, implying that lipolysis is central to BAT thermogenesis (40). Although it seems clear that BAT relies on lipids to fuel thermogenesis during cold

**TABLE 4**  
Additional Baseline Serum Metabolite *t* Test and Regression Analysis Results

Metabolite	BAT <sub>low</sub>		BAT <sub>high</sub>		<i>r</i>		<i>P</i>
	$\mu$	$\sigma$	$\mu$	$\sigma$	BMV	SUL <sub>max</sub>	
TSH ( $\mu$ IU/mL)	1.6	0.7	2.8	2.1	0.52	0.64	0.002
Sodium (mmol/L)	141.0	1.8	139.0	1.3	-0.40	-0.39	<0.001
Potassium (mmol/L)	3.8	0.3	4.0	0.3	0.31	0.26	0.002
Chloride (mmol/L)	102.5	2.1	103.3	3.0	0.14	0.31	0.329
CO <sub>2</sub> (mmol/L)	26.0	1.7	25.9	2.1	0.07	-0.14	0.964
Anion gap (mmol/L)	12.4	2.4	9.7	1.8	-0.51	-0.53	<0.001
Blood urea nitrogen (mg/dL)	13.2	2.8	10.7	2.2	-0.43	-0.50	<0.001
Creatinine (mg/dL)	0.8	0.1	0.8	0.1	0.14	-0.08	0.654
Calcium (mg/dL)	9.4	0.5	9.3	1.0	-0.05	-0.13	0.454
Bilirubin (mg/dL)	0.6	0.3	0.4	0.3	-0.30	-0.37	0.447
Protein (g/dL)	7.5	0.5	7.1	0.4	-0.41	-0.46	0.002
Albumin (g/dL)	4.6	0.3	4.3	0.3	-0.49	-0.54	<0.001
Alkaline phosphatase (U/L)	57.3	17.3	45.2	13.7	-0.35	-0.44	<0.001
Alanine aminotransferase (U/L)	18.3	4.4	34.0	26.4	0.53	0.24	0.006
Aspartate transaminase (U/L)	21.9	4.2	29.7	12.8	0.58	0.32	0.006

*P* values were generated using unpaired *t* tests comparing BAT<sub>high</sub> and BAT<sub>low</sub> groups. Using Bonferroni adjustment, *P* < 0.003 was considered significant.

exposure, most studies have not found a corresponding increase in serum or plasma lipid levels (8,14,19). One possible explanation for the significant increases we found in circulating lipid levels is that activated BMVs elicited in this study were considerably higher than in most other published work. A higher degree of activation would likely deplete intracellular fuel and require additional substrates from other sources. This type of control mechanism over triglyceride metabolism via clearance by BAT has been demonstrated in cold-exposed mice (12).

#### Early Metabolic Dysfunction

Orava et al. found BAT to be highly sensitive to stimulation by insulin (35). In young, healthy adults, it may be the case that higher insulin levels result in routine activation of BAT, which has been shown to increase overall BMV (15,41). Free fatty acids, derived from triglyceride lipolysis, are thought to be activators of uncoupling protein 1. We found higher thermoneutral circulating triglyceride levels in subjects with greater volumes of BAT. This may be another mechanism of routine BAT activation. Additionally, baseline plasma TSH was found to be significantly elevated in subjects with higher amounts of cold-activated BAT. TSH receptors are present in adipose tissue and have been linked to an increase in uncoupling protein 1 expression in preadipocytes (42). This may indicate that increased TSH levels stimulate BAT production. These findings, along with the strong positive correlations between BMV and thermoneutral insulin, glucose, and triglyceride levels, may suggest BAT plays a role in protecting against early stages of insulin resistance (preprediabetes) and hyperlipidemias.

#### Metabolic Profile

Previous studies have tended to show that activated BAT is associated with a healthier metabolic profile (i.e., lower fasting

glucose, greater insulin sensitivity, and less likelihood of diabetes, obesity, and cardiometabolic diseases) (16–18,22,37). The results of our study show that within a group of young, lean, healthy adults, those with a higher BMV had a potentially poorer overall metabolic profile. Higher baseline insulin, glucose, TSH, and serum triglycerides were associated with a higher BMV. Those with less activated BAT also exercised more (about twice as much per week) and were more likely to report adhering to diets that could be considered healthier. The effect of exercise on BAT is unclear in humans, as relevant studies have produced conflicting results. However, exercise is known to cause secretion of endocrine factors that modulate BAT activity, including cardiac natriuretic peptides (induction of uncoupling protein 1 expression and mitochondrial biogenesis) (43), fibroblast growth factor 21 (increased BAT activity) (44), and interleukin 6 (improved BAT-mediated metabolic homeostasis) (13).

Dietary differences are particularly interesting, as certain diet regimens likely include foods known to contain BAT-promoting compounds (45). At least part of a vegetarian or vegan diet may contain foods rich in phytochemicals such as capsaicin (46) or curcumin (47), which have been linked to increased BAT activation. There is also accumulating evidence that eicosapentaenoic acid and docosahexaenoic acid, found abundantly in fish oils (a likely component of a pescatarian diet), may stimulate BAT thermogenesis (48) and WAT browning (49). It may be somewhat surprising, then, that all but one subject who reported adhering to a strict dietary regimen were part of the BAT<sub>low</sub> group. It may be the case that the high BMV exhibited by subjects in the BAT<sub>high</sub> group who exercised less and consumed less healthy diets played a protective role against the early symptoms of metabolic disorders, which are driven at least in part by lifestyle choices.

## Adipokines Released from BAT (BATokines)

Although BAT is hypothesized to shift caloric balance in a net-negative direction, its endocrine effects may be more potent. In animal models, BAT transplants can improve glucose tolerance, increase whole-body insulin sensitivity, and reverse type 1 diabetes (13,25,50). These improvements are unlikely the result of caloric expenditure or glucose consumption alone but appear to be caused by BAT endocrine signaling (51). BATokines are substances preferentially released by BAT versus WAT, which may have endocrine effects (52). BAT is known to release significant amounts of fibroblast growth factor 21 (53,54), which has a role in improving glucose intolerance and increasing fatty acid oxidation in the liver (55). An increase in insulin-like growth factor 1 is thought to be mostly responsible for the reversal of diabetes seen in mouse models (56). Neuregulin 4 is highly expressed in BAT and its overexpression correlates with improved glucose tolerance and decreased insulin insensitivity (57). BATokines such as these, which are potentially released routinely in people such as those in the BAT<sub>high</sub> group, may help to mitigate the impacts of early metabolic or hormonal disturbances.

It is important to note that although significant differences in metabolite levels were found between groups with higher and lower activated BAT volumes, almost all metabolite levels detected during this study were within reference ranges. In otherwise healthy individuals, such as those studied here, who present with borderline metabolic results (e.g., upper end of the normal range of insulin or glucose) it would be useful to correlate their levels of BAT activity with clinical outcomes over time. It may also be beneficial to collect additional samples at subsequent time points to assess the short-term impact of cooling and BAT activation on lipid and other metabolite levels.

## CONCLUSION

Our data, obtained under conditions that strongly activate BAT, show significant systemic differences between individuals with higher and lower volumes of active BAT. From these data, we believe that BAT may be recruited to counteract incipient prepre-diabetic states, potentially serving as a first-line protective mechanism against very early metabolic and hormonal variations.

## DISCLOSURE

No potential conflict of interest relevant to this article was reported.

## ACKNOWLEDGMENTS

The work presented here was conducted using the scanning and special services in the MIR Center for Clinical Imaging Research, located at the Washington University Medical Center. We thank Lauren Ash, Jessica Cartier, and Lisa Schmidt for assistance with data collection.

## KEY POINTS

**QUESTION:** Is active BAT associated with a particular metabolic profile in healthy, young adults?

**PERTINENT FINDINGS:** In a young, otherwise healthy sample of adults, a higher volume of active BAT was found to be associated with significantly higher preactivation levels of serum glucose, insulin, TSH, and triglycerides.

**IMPLICATIONS FOR PATIENT CARE:** Imaging BAT using <sup>18</sup>F-FDG PET/CT may help identify patients with very early metabolic abnormalities.

## REFERENCES

1. Klepac K, Georgiadi A, Tschop M, Herzog S. The role of brown and beige adipose tissue in glycaemic control. *Mol Aspects Med.* 2019;68:90–100.
2. Cannon B, Nedergaard J. Brown adipose tissue: function and physiological significance. *Physiol Rev.* 2004;84:277–359.
3. Hany TF, Gharehpapagh E, Kamel EM, Buck A, Himms-Hagen J, von Schulthess GK. Brown adipose tissue: a factor to consider in symmetrical tracer uptake in the neck and upper chest region. *Eur J Nucl Med Mol Imaging.* 2002;29:1393–1398.
4. Cohade C, Osman M, Panu HK, Wahl RL. Uptake in supraclavicular area fat (“USA-Fat”): description on <sup>18</sup>F-FDG PET/CT. *J Nucl Med.* 2003;44:170–176.
5. Chen KY, Cypess AM, Laughlin MR, et al. Brown Adipose Reporting Criteria in Imaging Studies (BARCIST 1.0): recommendations for standardized FDG-PET/CT experiments in humans. *Cell Metab.* 2016;24:210–222.
6. Chondronikola M, Beeman SC, Wahl RL. Non-invasive methods for the assessment of brown adipose tissue in humans. *J Physiol (Lond).* 2018;596:363–378.
7. Cypess AM, Lehman S, Williams G, et al. Identification and importance of brown adipose tissue in adult humans. *N Engl J Med.* 2009;360:1509–1517.
8. Ouellet V, Labbe SM, Blondin DP, et al. Brown adipose tissue oxidative metabolism contributes to energy expenditure during acute cold exposure in humans. *J Clin Invest.* 2012;122:545–552.
9. Coolbaugh CL, Damon BM, Bush EC, Welch EB, Towse TF. Cold exposure induces dynamic, heterogeneous alterations in human brown adipose tissue lipid content. *Sci Rep.* 2019;9:13600.
10. Blondin DP, Nielsen S, Kuipers EN, et al. Human brown adipocyte thermogenesis is driven by  $\beta$ 2-AR stimulation. *Cell Metab.* 2020;32:287–300.e7.
11. Albert V, Svensson K, Shimobayashi M, et al. mTORC2 sustains thermogenesis via Akt-induced glucose uptake and glycolysis in brown adipose tissue. *EMBO Mol Med.* 2016;8:232–246.
12. Bartelt A, Bruns OT, Reimer R, et al. Brown adipose tissue activity controls triglyceride clearance. *Nat Med.* 2011;17:200–205.
13. Stanford KI, Middelbeek RJ, Townsend KL, et al. Brown adipose tissue regulates glucose homeostasis and insulin sensitivity. *J Clin Invest.* 2013;123:215–223.
14. Iwen KA, Backhaus J, Cassens M, et al. Cold-induced brown adipose tissue activity alters plasma fatty acids and improves glucose metabolism in men. *J Clin Endocrinol Metab.* 2017;102:4226–4234.
15. Blondin DP, Labbe SM, Tingelstad HC, et al. Increased brown adipose tissue oxidative capacity in cold-acclimated humans. *J Clin Endocrinol Metab.* 2014;99:E438–E446.
16. Ouellet V, Routhier-Labadie A, Bellemare W, et al. Outdoor temperature, age, sex, body mass index, and diabetic status determine the prevalence, mass, and glucose-uptake activity of <sup>18</sup>F-FDG-detected BAT in humans. *J Clin Endocrinol Metab.* 2011;96:192–199.
17. Jacene HA, Cohade CC, Zhang Z, Wahl RL. The relationship between patients’ serum glucose levels and metabolically active brown adipose tissue detected by PET/CT. *Mol Imaging Biol.* 2011;13:1278–1283.
18. Becher T, Palanisamy S, Kramer DJ, et al. Brown adipose tissue is associated with cardiometabolic health. *Nat Med.* 2021;27:58–65.
19. Blondin DP, Labbe SM, Phoenix S, et al. Contributions of white and brown adipose tissues and skeletal muscles to acute cold-induced metabolic responses in healthy men. *J Physiol (Lond).* 2015;593:701–714.
20. Chondronikola M, Volpi E, Borsheim E, et al. Brown adipose tissue improves whole-body glucose homeostasis and insulin sensitivity in humans. *Diabetes.* 2014;63:4089–4099.
21. Chondronikola M, Volpi E, Borsheim E, et al. Brown adipose tissue activation is linked to distinct systemic effects on lipid metabolism in humans. *Cell Metab.* 2016;23:1200–1206.
22. Wang Q, Zhang M, Xu M, et al. Brown adipose tissue activation is inversely related to central obesity and metabolic parameters in adult human. *PLoS One.* 2015;10:e0123795.
23. Berbée JF, Boon MR, Khedoe PP, et al. Brown fat activation reduces hypercholesterolaemia and protects from atherosclerosis development. *Nat Commun.* 2015;6:6356.
24. Schlein C, Talukdar S, Heine M, et al. FGF21 lowers plasma triglycerides by accelerating lipoprotein catabolism in white and brown adipose tissues. *Cell Metab.* 2016;23:441–453.
25. Gunawardana SC, Piston DW. Reversal of type 1 diabetes in mice by brown adipose tissue transplant. *Diabetes.* 2012;61:674–682.
26. Blondin DP, Tingelstad HC, Noll C, et al. Dietary fatty acid metabolism of brown adipose tissue in cold-acclimated men. *Nat Commun.* 2017;8:14146.
27. U Din M, Saari T, Raiko J, et al. Postprandial oxidative metabolism of human brown fat indicates thermogenesis. *Cell Metab.* 2018;28:207–216.e3.
28. Fraum TJ, Crandall JP, Ludwig DR, et al. Repeatability of quantitative brown adipose tissue imaging metrics on positron emission tomography with <sup>18</sup>F-fluorodeoxyglucose in humans. *Cell Metab.* 2019;30:212–224.e4.

29. Cohade C, Mourtzikos KA, Wahl RL. "USA-Fat": prevalence is related to ambient outdoor temperature-evaluation with <sup>18</sup>F-FDG PET/CT. *J Nucl Med.* 2003;44:1267–1270.
30. Saito M, Okamatsu-Ogura Y, Matsushita M, et al. High incidence of metabolically active brown adipose tissue in healthy adult humans: effects of cold exposure and adiposity. *Diabetes.* 2009;58:1526–1531.
31. Baba S, Tatsumi M, Ishimori T, Lilien DL, Engles JM, Wahl RL. Effect of nicotine and ephedrine on the accumulation of <sup>18</sup>F-FDG in brown adipose tissue. *J Nucl Med.* 2007;48:981–986.
32. Graham MM, Wahl RL, Hoffman JM, et al. Summary of the UPICT protocol for <sup>18</sup>F-FDG PET/CT imaging in oncology clinical trials. *J Nucl Med.* 2015;56:955–961.
33. Kinahan PE, Perlman ES, Sunderland JJ, et al. The QIBA profile for FDG PET/CT as an imaging biomarker measuring response to cancer therapy. *Radiology.* 2020;294:647–657.
34. Tahari AK, Chien D, Azadi JR, Wahl RL. Optimum lean body formulation for correction of standardized uptake value in PET imaging. *J Nucl Med.* 2014;55:1481–1484.
35. Orava J, Nuutila P, Lidell ME, et al. Different metabolic responses of human brown adipose tissue to activation by cold and insulin. *Cell Metab.* 2011;14:272–279.
36. Weir G, Ramage LE, Akyol M, et al. Substantial metabolic activity of human brown adipose tissue during warm conditions and cold-induced lipolysis of local triglycerides. *Cell Metab.* 2018;27:1348–1355.e4.
37. Lee P, Greenfield JR, Ho KK, Fulham MJ. A critical appraisal of the prevalence and metabolic significance of brown adipose tissue in adult humans. *Am J Physiol Endocrinol Metab.* 2010;299:E601–E606.
38. Persichetti A, Sciuto R, Rea S, et al. Prevalence, mass, and glucose-uptake activity of <sup>18</sup>F-FDG-detected brown adipose tissue in humans living in a temperate zone of Italy. *PLoS One.* 2013;8:e63391.
39. Din MU, Raiko J, Saari T, et al. Human brown fat radiodensity indicates underlying tissue composition and systemic metabolic health. *J Clin Endocrinol Metab.* 2017;102:2258–2267.
40. Blondin DP, Frisch F, Phoenix S, et al. Inhibition of intracellular triglyceride lipolysis suppresses cold-induced brown adipose tissue metabolism and increases shivering in humans. *Cell Metab.* 2017;25:438–447.
41. van der Lans AA, Hoeks J, Brans B, et al. Cold acclimation recruits human brown fat and increases nonshivering thermogenesis. *J Clin Invest.* 2013;123:3395–3403.
42. Zhang L, Baker G, Janus D, Paddon CA, Fuhrer D, Ludgate M. Biological effects of thyrotropin receptor activation on human orbital preadipocytes. *Invest Ophthalmol Vis Sci.* 2006;47:5197–5203.
43. Hansen D, Meeusen R, Mullens A, Dendale P. Effect of acute endurance and resistance exercise on endocrine hormones directly related to lipolysis and skeletal muscle protein synthesis in adult individuals with obesity. *Sports Med.* 2012;42:415–431.
44. Hanssen MJ, Broeders E, Samms RJ, et al. Serum FGF21 levels are associated with brown adipose tissue activity in humans. *Sci Rep.* 2015;5:10275.
45. Okla M, Kim J, Koehler K, Chung S. Dietary factors promoting brown and beige fat development and thermogenesis. *Adv Nutr.* 2017;8:473–483.
46. Yoneshiro T, Aita S, Kawai Y, Iwanaga T, Saito M. Nonpungent capsaicin analogs (capsinoids) increase energy expenditure through the activation of brown adipose tissue in humans. *Am J Clin Nutr.* 2012;95:845–850.
47. Wang S, Wang X, Ye Z, et al. Curcumin promotes browning of white adipose tissue in a norepinephrine-dependent way. *Biochem Biophys Res Commun.* 2015;466:247–253.
48. Oudart H, Groscolas R, Calgari C, et al. Brown fat thermogenesis in rats fed high-fat diets enriched with n-3 polyunsaturated fatty acids. *Int J Obes Relat Metab Disord.* 1997;21:955–962.
49. Zhao M, Chen X. Eicosapentaenoic acid promotes thermogenic and fatty acid storage capacity in mouse subcutaneous adipocytes. *Biochem Biophys Res Commun.* 2014;450:1446–1451.
50. Liu X, Zheng Z, Zhu X, et al. Brown adipose tissue transplantation improves whole-body energy metabolism. *Cell Res.* 2013;23:851–854.
51. White JD, Dewal RS, Stanford KI. The beneficial effects of brown adipose tissue transplantation. *Mol Aspects Med.* 2019;68:74–81.
52. Lee MW, Lee M, Oh KJ. Adipose tissue-derived signatures for obesity and type 2 diabetes: adipokines, batokines and microRNAs. *J Clin Med.* 2019;8:854.
53. Chartoumpakis DV, Habeos IG, Ziros PG, Psyrogiannis AI, Kyriazopoulou VE, Papavassiliou AG. Brown adipose tissue responds to cold and adrenergic stimulation by induction of FGF21. *Mol Med.* 2011;17:736–740.
54. Di Franco A, Guasti D, Squecco R, et al. Searching for classical brown fat in humans: Development of a novel human fetal brown stem cell model. *Stem Cells.* 2016;34:1679–1691.
55. Fisher FM, Maratos-Flier E. Understanding the physiology of FGF21. *Annu Rev Physiol.* 2016;78:223–241.
56. Gunawardana SC, Piston DW. Insulin-independent reversal of type 1 diabetes in nonobese diabetic mice with brown adipose tissue transplant. *Am J Physiol Endocrinol Metab.* 2015;308:E1043–E1055.
57. Wang G-X, Zhao X-Y, Meng Z-X, et al. The brown fat-enriched secreted factor Nrg4 preserves metabolic homeostasis through attenuation of hepatic lipogenesis. *Nat Med.* 2014;20:1436–1443.